

## IN-CYLINDER FLOW ANALYSIS OF DIFFERENT VALVE LIFT USING CFD<sup>1</sup>

Victor IORGA-SIMAN<sup>1,2</sup>; Adrian CLENCI<sup>1,2\*</sup>; Pierre PODEVIN<sup>2</sup>; Alain DELACROIX<sup>2</sup>; Ion TABACU<sup>1</sup>

<sup>1</sup>University of Pitesti, Romania, <sup>2</sup>Conservatoire National des Arts et Métiers Paris, France

**Abstract:** *As it is well known, the variable valve actuation (VVA) enables added control of valve timing, lift and/or duration. With this additional freedom, the efficiency of an engine can be greatly increased. Not only can the compression ratio be increased with the addition of VVA, but also the necessity of throttling can be reduced, [13] This paper presents a variable intake valve lift (ViVL) mechanism, used to enhance fuel economy. Two operational, in-line, 4 cylinders engines prototypes are working on the test benches: one is a side mounted camshaft and overhead valves (OHV) version (i.e. a pushrod engine), still being built in some countries and the other is an overhead camshaft (OHC) version. Experiments that proved also their ability for the unthrottled operation have been conducted on the engine test bench. A CFD study on the airflow was launched using the numerical code ANSYS-Fluent in order to get more information about the phenomenon happening during the intake stroke of our prototype ViVL engine. To simulate the turbulent flow which takes place during the air induction,  $k-\varepsilon$  realizable turbulent model was chosen. This investigation present results from a 3D numerical simulation of the air flow at an engine speed of 800 rpm, corresponding to the idle operation. For one opening of throttle plate (21.6°) and different valve lifts laws, the purpose was to obtain results about cylinder pressure and air velocity. Also, using the path-lines technique, the visualization of swirl motion is highlighted in this paper.*

**Keywords:** variable intake valve lift ViVL, CFD, 3D model, flow field visualization, swirl motion, intake flow velocity

### INTRODUCTION

The purpose of internal combustion engines is the production of mechanical power from the chemical energy contained the fuel. In internal combustion engine, this energy is released by burning or oxidizing the fuel inside the engine. The fuel-air mixture before combustion and the burned products after combustion are the actual working fluid, [10]

In an internal combustion engine, there are tree main factors that influence each others: performance, fuel economy and emissions. Those three factors could be improved for different engine operating points. The analyses of the urban driving cycles of NEDC reveal that the weight of idle and average engine speed is significant. In a spark ignition engine, these operating condition are achieved by small and moderate openings of throttle plate, which generates additional losses during the intake stroke. In these operating points, the engine efficiency decreases from the peak values (already not very high) to values dramatically lower.

The introduction of a VVA system provides significant improvement at part loads operation, [1, 3, 4, 5]. For instance, the ability to control valve lift certainly offers the ability to control intake air mass (see throttle-less operation) but also has the added benefit that it improves fuel-air mixing process and controls air motion. This is particularly important at idle and low part loads when low lifts are to be used for improving the engine's fuel economy or for achieving the required power, [1, 3, 6,]

In this study, a computational fluid dynamics (CFD) simulation, using ANSYS-Fluent, is performed to analyze the effect of different valve lift laws over the filling process and fluid motion. In-cylinder motion

---

<sup>1</sup> <sup>1</sup>This article was produced under the project "Supporting young Ph.D students with frequency by providing doctoral fellowships", co-financed from the EUROPEAN SOCIAL FUND through the Sectorial Operational Program Development of Human Resources

\* Corresponding author. Email: adi.clenci@upit.ro

is commonly divided in two types: swirl and tumble. Swirl is the rotational movement of the charge around the cylinder axis, while tumble is the movement of the cylinder charge from the upside to the down side of the cylinder regions and back again, around an axis perpendicular to the cylinder axis, [12]. For the numerical simulation, a 3D transient approach was chosen.

### ViVL MECHANISM DESCRIPTION

In context of fuel economy, the authors focus is on the ViVL technique used to enhance fuel consumption in the idle and low part loads operation. Two operational 4 cylinder engines prototypes able to continuously vary iVL are working on the test benches within the University of Pitesti: one is a side mounted camshaft and overhead valves (OHV) version, 1.4 liters displacement and the other is an overhead camshaft (OHC) version, 1.6 liters. Both of them feature MPI and 2 valves per cylinder. Experiments that proved also their ability for the unthrottled operation have been conducted on the engine test bench, [2].

The ViVL mechanism presented in this paper is overhead valves (OHV). As seen from figure 1, it is about a push-rod/rocker type mechanism, able to adjust the intake valve lift thanks to an assembly consisting in an oscillating follower and a translational skate. The skate's position on the follower is adjusted with the help of a connecting rod and a control lever, so that every intake valve lift can be achieved continuously between minimum and maximum value during operation. Currently, the control lever's position is given by a hydraulic cylinder, fed with oil from the engine's main oil gallery, this hydraulic cylinder being attached to the engine, [3, 5, 9].

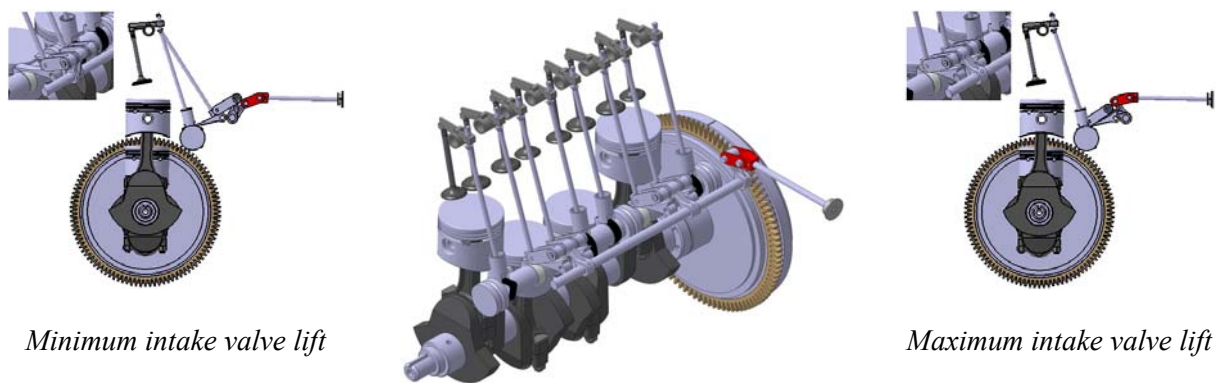


Figure 1. The OHV ViVL mechanism

The mechanism studied is able to generate several valve lift laws, for some different positions of the control lever. Shapes of few valves lift laws measured at the test bench are highlighted in figure 2. In the same figure, the piston velocity and exhaust valve law are shown.

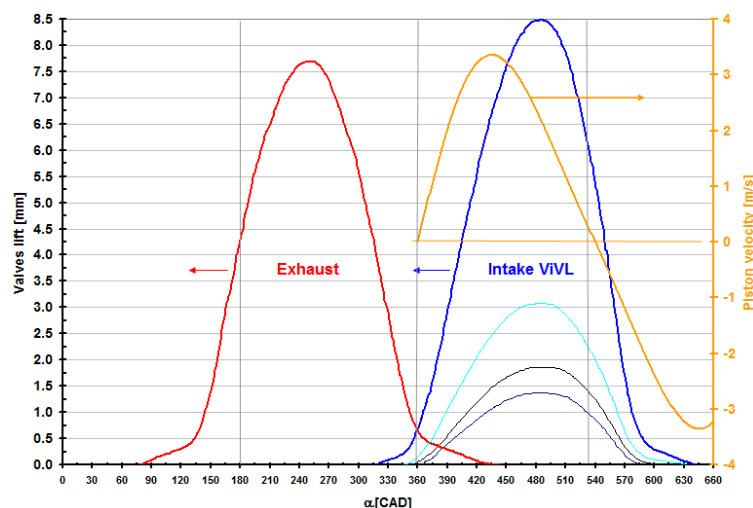


Figure 2. (continued)

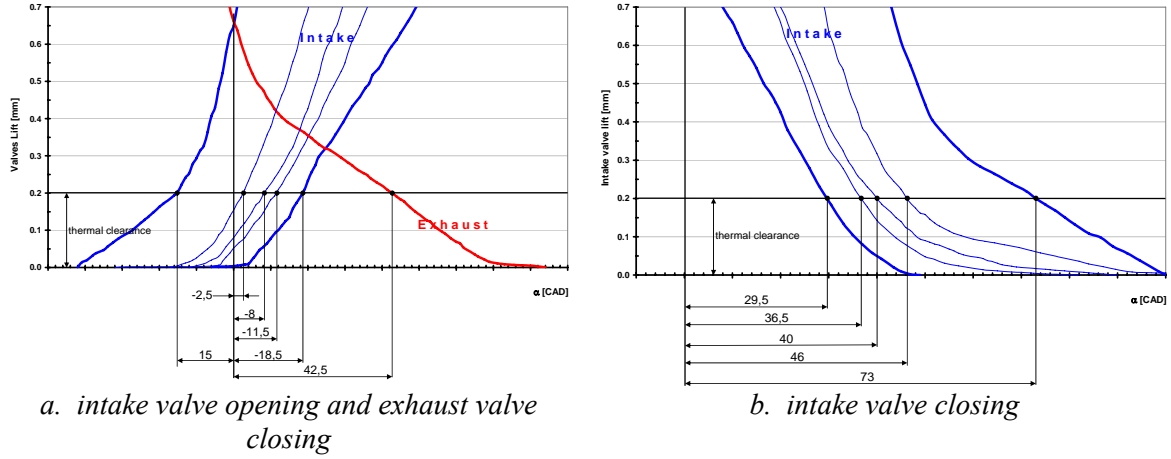


Figure 2. The valve actuation diagram

## CFD SIMULATION DISCRIPTION

Performing experiments on an engine is sometimes difficult because of its complexity, especially when flow measurements need to be involved. Numerical experiments have the advantage that an expensive and time consuming measurement set-up is not necessary.

Dynamic simulation of fluid flow in ViVL prototype engine were performed at 800 rpm corresponding to the idle operation. The CFD simulation was carried out at 3D level with a finite volume commercial program, ANSYS-Fluent. Implicit solver and *realizable k-ε* turbulence model for high Reynolds numbers with standard wall function were used for closure.

### Realizable k-ε model description

The *realizable k-ε* model is a relatively recent development and differs from the standard *k-ε* model in two important ways:

- The *realizable k-ε* model contains a new formulation for the turbulent viscosity.
- A new transport equation for the dissipation rate,  $\varepsilon$ , has been derived from an exact equation for the transport of the mean-square vorticity fluctuation.

The term “*realizable*” means that the model satisfies certain mathematical constraints on the Reynolds stresses, consistent with the physics of turbulent flows. Neither the standard *k-ε* model nor the *RNG k-ε* model is realizable, [14]

The modeled transport equations for  $k$  and  $\varepsilon$  in the *realizable k-ε* model are:

$$\frac{\partial}{\partial t}(\rho k) + \frac{\partial}{\partial x_j}(\rho k u_j) = \frac{\partial}{\partial x_j} \left[ \left( \mu + \frac{\mu_t}{\sigma_k} \right) \frac{\partial k}{\partial x_j} \right] + G_k - \rho \varepsilon \quad (1)$$

$$\frac{\partial}{\partial t}(\rho \varepsilon) + \frac{\partial}{\partial x_i}(\rho \varepsilon \bar{u}_i) = \frac{\partial}{\partial x_j} \left[ \left( \mu + \frac{\mu_t}{\sigma_\varepsilon} \right) \frac{\partial \varepsilon}{\partial x_j} \right] + \rho C_1 S \varepsilon - \rho C_2 \frac{\varepsilon^2}{k + \sqrt{v \varepsilon}} \quad (2)$$

where:  $C_1 = \max \left[ 0.43 \frac{\eta}{\eta + 5} \right]$ ,  $\eta \equiv S \frac{k}{\varepsilon}$ ,  $S = \sqrt{2 S_{ij} S_{ij}}$

The equation for the kinetic energy has the same expression as the standard and *RNG k-ε* models. Only the equation for the dissipation rate is quite different. As in other *k-ε* models, the eddy viscosity is computed from:

$$\mu_t = \rho C_\mu \frac{k^2}{\varepsilon} \quad (3)$$

The difference between the *realizable k-ε* model and the standard and *RNG k-ε* models is that  $C_\mu$  is no longer constant. It is computed from:

$$C_\mu = \frac{1}{A_0 + A_s k U^* / \varepsilon} \quad (4)$$

where:  $U^* \equiv \sqrt{S_{ij}S_{ij} + \tilde{\Omega}_{ij}\tilde{\Omega}_{ij}}$ ,  $\tilde{\Omega}_{ij} = \bar{\Omega}_{ij} = \frac{1}{2} \left( \frac{\partial \bar{u}_j}{\partial x_i} - \frac{\partial \bar{u}_i}{\partial x_j} \right)$

where  $A_0$  and  $A_s$  are constants and  $\bar{\Omega}_{ij}$  is the mean rate of rotation tensor. It can be seen that  $C_\mu$  is a function of the mean strain and rotation rates, the angular velocity of the systems rotation and the turbulence fields ( $k$  and  $\varepsilon$ ). The turbulent viscosity is dependent of the direction and is therefore anisotropic, [14]

### 3D Model Geometry

This type of model used for calculating the numerical simulation keeps the geometrical characteristics of the real engine studied. Taking as a starting point geometry built using CATIA V5R19, were kept only certain components which ensure the filling process, materialized in: throttle body, throttle plate, a part of the intake manifold, cylinder head intake channel, intake valve, exhaust valve, cylinder head exhaust channel, combustion chamber, cylinder and piston (figure 3).

Basic dimensions of the 3D model are displayed in following table.

Table 1. Geometry dimensions

Throttle body diameter [mm]	63.5
Manifold diameter [mm]	29.53
Intake valve diameter [mm]	33.2
Length of intake valve seat [mm]	2.81
Exhaust valve diameter [mm]	30
Length of exhaust valve seat [mm]	1.41
Bore [mm]	76
Stroke [mm]	77
Connecting rod length[mm]	128
Intake valve angle [°]	45
Compression ratio[-]	8.5

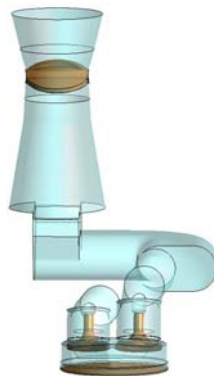


Figure 3. (continued)



Figure 3. Geometry model

### Mesh generation and Numerical simulation

Importing the geometry of the engine into pre-processor Gambit and make it suitable for simulation, was the next step after the model was built. After that, it was necessary to clean the geometry (eliminate unneeded vertices, edges and planes) and complete the gap between the different shapes.

The computational domain was divided in about 15 volumes. Each volume has been meshed separately with unstructured and structured discretization schema. Hexahedral cells and structured grid have been used for generate the mesh above the piston, intake and exhaust valve. Unstructured grids with tetrahedral cells form the rest of calculation domain. In the combustion chamber, the unstructured mesh is only necessary for the opening and closing of the valves because the grid has to be re-meshed to avoid degenerated grid cells. The tetrahedral unstructured grid in combination with a second-order discretization scheme gives similar results in case of the *realizable k-ε* turbulence model. Grid resolution measured is  $y^+ = 50$ , sufficient for the use of standard wall function. For moving parts, two valves which move on YZ direction and one piston move to Z direction. The number of cells varies from 825465 cells at TDC and 1188420 cells at BDC, for the maximum valve law (8.47 mm maximum intake valve lift); 1185605 for the minimum valve lift law (1.365 mm minimum intake valve lift)

There are three methods to update the meshes of a moving boundary project: smoothing, re-meshing and layering. For tetrahedral cells (combustion chamber), smoothing method was used. Re-meshing method is after the smoothing method and generates new layers when tetrahedral cells exist. Layering method is suitable for hexahedral cells in cylinder zone.

Pressure inlet is one boundary condition above the throttle plate. The pressure outlet was chosen as boundary condition at the end of exhaust manifold. A constant pressure of 98000 was assigned in all computational volume. In order to calculate the effects of compressibility, in the whole computational domain, an inert gas with the properties of air was considered and the entire walls were considered adiabatic. Several simulation conditions are shown in table 2.

Table 2: Model characteristic constants

Temperature	300[K]
Cp (Specific Heat)	1006.43 [ $J / kg \cdot K$ ]
Thermal conductivity	0.0242 [ $W / m \cdot ^\circ C$ ]
Viscosity	$1.7894 \cdot 10^{-5}$ [ $kg / m \cdot s$ ]
Engine speed	800 [rot/min]
Crank angle step size	0.5 [CAD]

### CALCULATION RESULTS AND DISCUSSION

Numerical simulation approached two cases

1. For a fixed opening of the throttle plate ( $\varphi=21.6^\circ$ ), the simulation was carried out with exhaust valve lift law and minimum intake valve lift law.

2. In the second case, the maximum valve lift law has been used at the same opening of the throttle plate ( $\varphi=21.6^\circ$ ) and the same exhaust valve lift laws

Valves laws characteristics are mentioned in table 4

Table 3. Durations and timings of the valves laws

	Min. intake valve lift law	Max. intake valve lift law	Exhaust valve lift law
Valve lift height[mm]	1.365	8.47	7.49
Valve opening time [CAD]	378	344	105
Valve closing time [CAD]	569	613	402
Valve Opening Advance [CAD]	-18	16	75
Valve Closing Retard [CAD]	29	73	42
Opening Duration [°CAD]	191	269	297

In-cylinder pressure during the progress of an engine cycle for the cases analyzed, is represented in figure 4

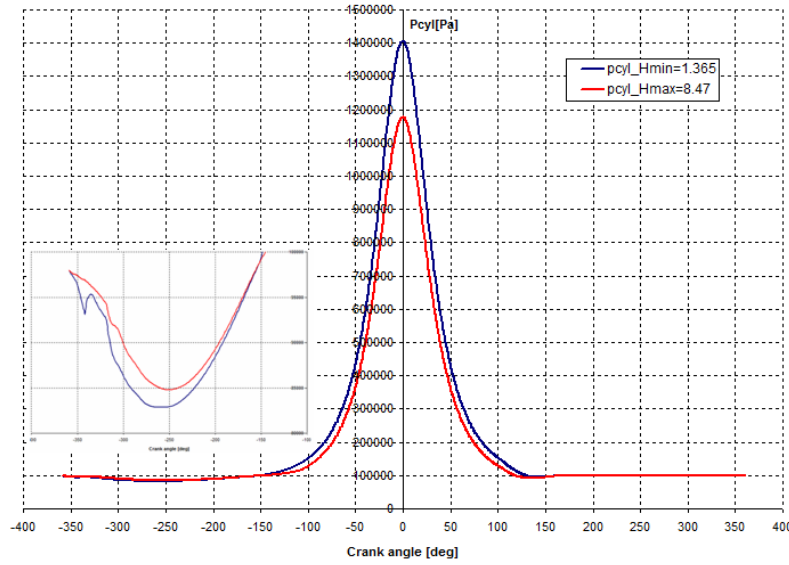


Figure 4. Cylinder pressure

Looking at the chart above can be observed that in-cylinder absolute pressure peaks measured when the throttle plate is open at 21.6 °, using maximum valve lift law (red line) and minimum valve lift law (line blue), are different. In the case of minimum valve lift law, the in cylinder pressure reaches a maximum of 13.8 bar. Instead for maximum lifting law the peak pressure does not exceed 11.9 bar.

One may notice in the previous figure that in spite of a higher pumping loss during the intake stroke at minimum valve law, the peak pressure is however higher. This could be explained by a higher effective compression ratio due to a lower delay in the closing of intake valve at minimum valve law (see table 3). In the case of maximum intake valve law, due to a higher delay for the intake valve closing, during the first part of compression stroke, before the intake valve closes, one may expect a reverse flow, from the cylinder to the intake manifold. Certainly, this will cause a lower peak pressure. On the other hand, it shouldn't be forgotten that the aforesaid are valid for an engine idling speed (800 rpm/min). When increasing the engine speed the results will change substantially.

In order to analyze the phenomenon of reverse flow motion, the following relation will be used:

$$P_{intake} = p_{col} - p_{cyl} = \Delta p \quad (5)$$

If  $\Delta p > 0 \Leftrightarrow p_{col} > p_{cyl} \Rightarrow$  normal flow

If  $\Delta p < 0 \Leftrightarrow p_{col} < p_{cyl} \Rightarrow$  reverse flow

where:  $p_{col}$  = intake manifold pressure,  $p_{cyl}$  = cylinder pressure

Following the relation 5, the difference in pressure between the intake manifold and the cylinder is displayed graphically in the figure 5 along with a picture that highlights the start of the reverse flow phenomenon.

One conclusion is that at the minimum valve lift law, the duration of reverse flows is smaller.

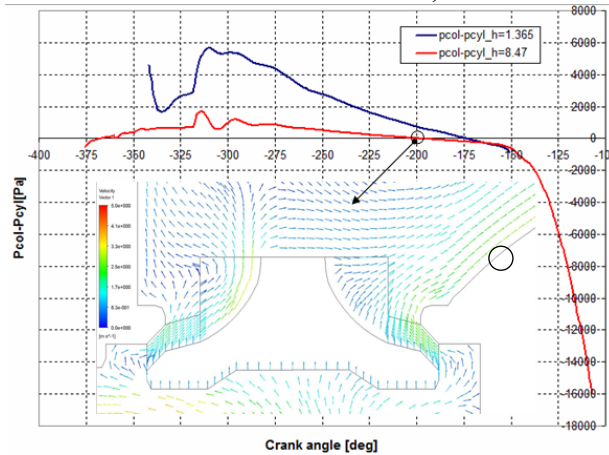


Figure 5. Evolution of  $\Delta p$  and the reverse flows

### Swirl Motion Analysis

The efficiency of an internal combustion engine depends in a high degree on the specifics of combustion. The quality of combustion is directly dependent on the oxygen-fuel mixing characteristic within the cylinder. It is therefore very important that the air-fuel mixture is as homogeneous as possible. In order to improve the level of homogeneity the in cylinder fluid rotation plays a significant role. If the fluid rotates around the axis of the cylinder, the motion is called swirl flow, and if the rotation is perpendicular to the axis it's tumbling flow, [7].

#### Swirl intensity

The mixing rotation or swirl intensity, depends on several factors, the most important of each are the position of the valve with respect to the axis of cylinder, the inlet geometry and the length of the valve stroke or angular position of the crank.

The swirl intensity is characterized by dimensionless number known as a swirl number. Swirl number has been defined as follows, [7]:

$$SN = \frac{\Gamma}{I \cdot 2 \cdot \pi \cdot rps} \quad (6)$$

where:  $\Gamma$  - angular momentum of fluid,  $I$  - moment of inertia of fluid,  $rps$  - engine speed [rev/s], [8]

Using the results of CFD simulations for different valve lift, the variation of swirl number calculated with the expression (6) is plotted in figure 6. It can be seen that the in-cylinder swirl ratio can be increased by reduction the maximum valve lift. When the intake valve reaches higher lift the mass flow rate in associated with angular momentum flow make possible to achieve the maximum swirl number.

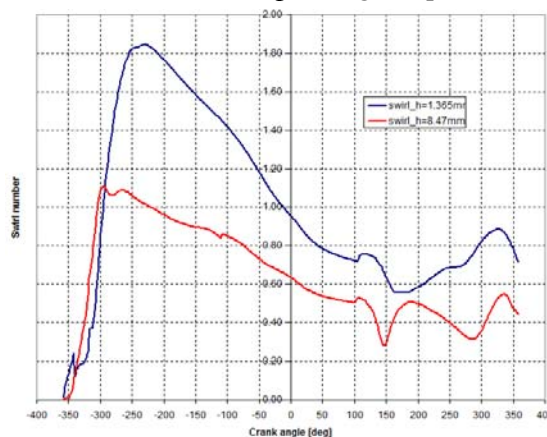
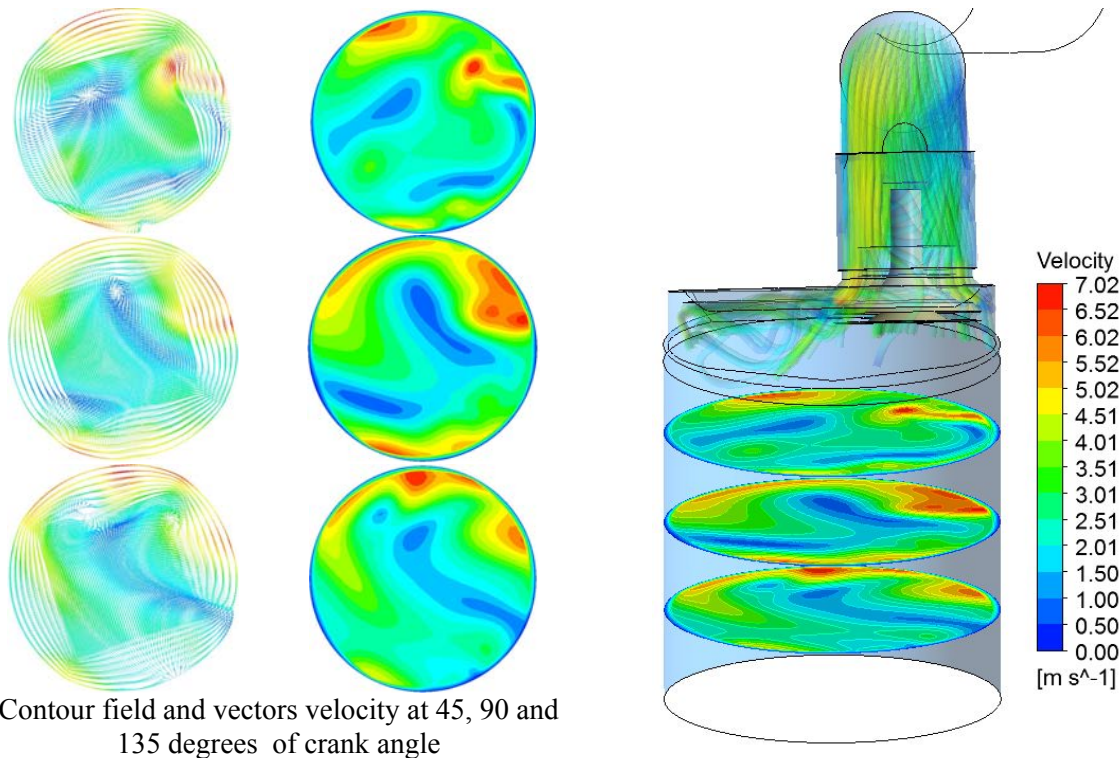
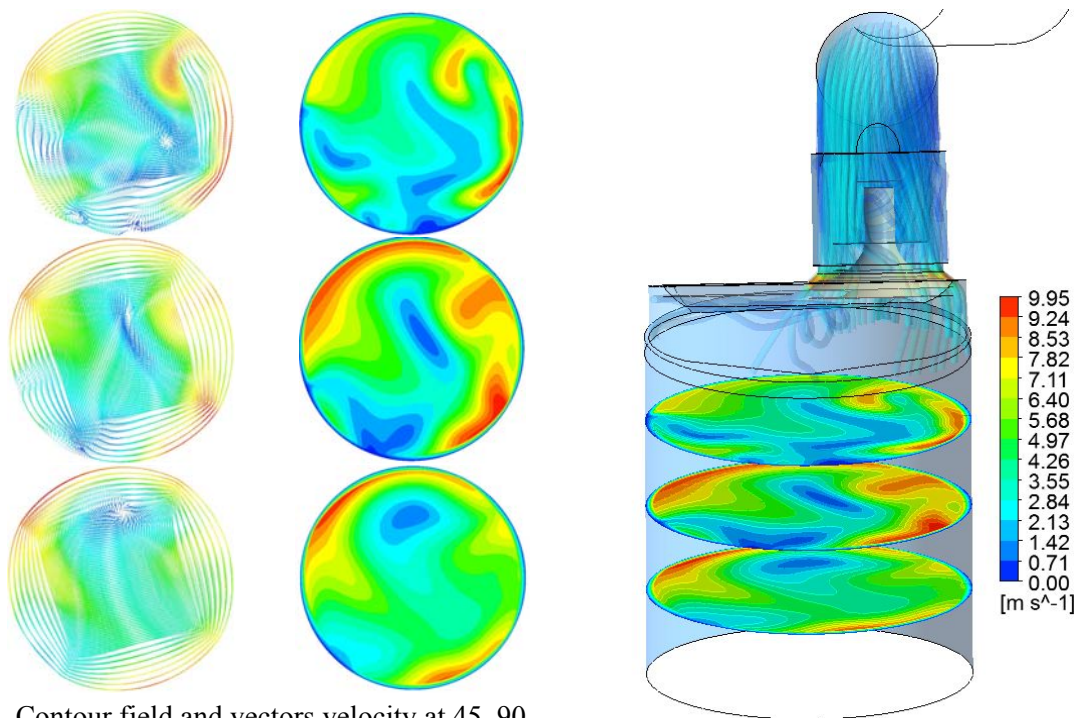


Figure 6. Calculated swirl number versus crank angle



Contour field and vectors velocity at 45, 90 and 135 degrees of crank angle

Figure 7. Swirl motion in different plane during intake stroke for maximum valve lift law  
The swirl motion for each case of valve lift law aforementioned, at different position of crank shaft, is reveal in figure 7 and figure 8



Contour field and vectors velocity at 45, 90 and 135 degrees of crank angle

Figure 8. Swirl motion in different plane during intake stroke for minimum valve lift law

The maximum flow velocity above the valve is reached at about 90 °CA where the piston instantaneous speed is maximal. After this, the velocity into cylinder decreases. For a good visualization of in-cylinder flow, the inside volume was cut with a plane parallel to the cylinder axis (figure 9, a). First, one may see that approaching the idle operation at 21.6° throttle plate opening with 1.365 mm maximum intake valve

lift is causing an increase in the velocity of intake flow at the valve gap. Its value is 103.4 m/s while at standard case is 41.9 m/s (figure 9, b and c).

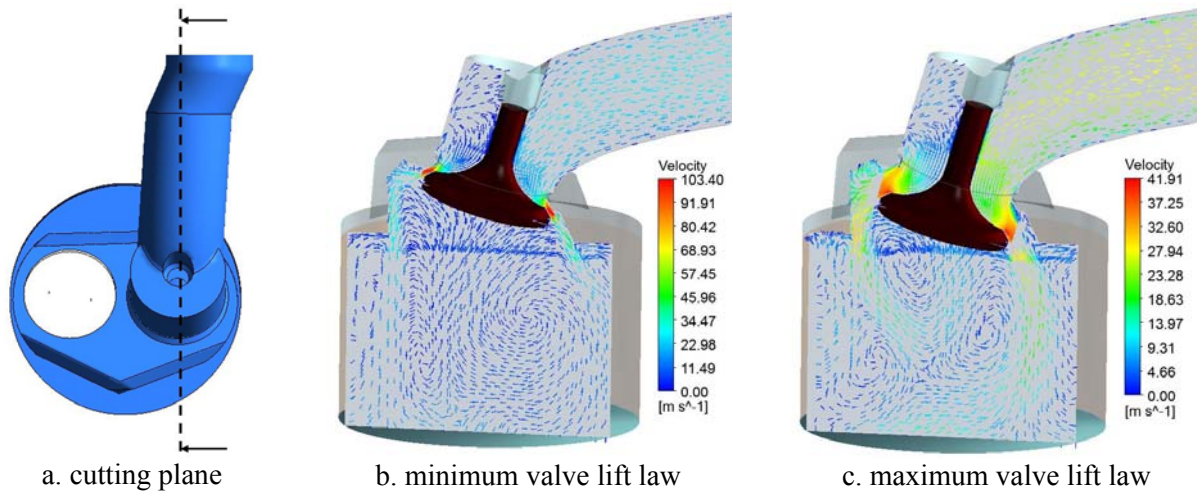


Figure 9. In cylinder velocity vectors at 90 CAD

## CONCLUSIONS

The reduction of fuel consumption is a fundamental aspect of the automotive industry. This comes from customers, as well as from legal demands. Variable valve actuation offers many opportunities to improve the spark ignition engine's performances in areas like fuel economy, emissions and power density and it seems it will become the next industry standard on gasoline engines

This study's goal was to obtain some insights about what's happening during the intake stroke of a variable intake valve lift prototype engine.

Three dimensional simulation and then visualization techniques, using streamlines, may also prove to be very useful because the in-cylinder flow motions inside the cylinder are difficult to visualize in the absence of performing technical equipment. In general, the optimal flow visualization technique depends on the needs of the user and the nature of vector field. It is possible to reveal and communicate different visualizing characteristic of the flow using 2D approach but in order to bring more light to the very complex in-cylinder flow phenomena, the using of the three dimensional CFD simulation is necessary

## REFERENCES

1. Bernhard, L. – *Less CO2 thanks to the BMW 4 cyl. Valvetronic engine*, ATA vol. 56, no 3-4/2003.
2. Bîzîiac A. – *Research regarding improving of energetic performance of a s.i.e featuring variable intake valve lift*, Doctoral Thesis, University of Pitești, 2011
3. Clenci, A., Bîzîiac, A., Berquez, J., Podevin, P., Descombes, G., Hara, V. - *Variable intake valve lift on spark ignition engine and the effects on fuel economy*, EAEC Congress, 2009, Bratislava, Slovakia
4. Clenci, A., Bîzîiac, A., Podevin, P., Descombes, G., Hara, V. - *Synthesis and analysis of a variable valve lift and timing mechanism*, 1<sup>st</sup> International Congress on Automotive, AMMA2007, held in Cluj-Napoca, Romania, under the patronage of FISITA.
5. Clenci, A., Podevin, P., Bîzîiac, A., Descombes, G., Hara, V. - *Development of a variable valve lift and timing system for low part loads efficiency improvement*, EAEC Congress, 2007, Budapest, Hungary
6. Clenci, A., Podevin, P. et al - *Moteur avec autorégulation de la levée des soupapes d'admission. Mise au point du système de contrôle de levée de soupapes*, Projet de recherche Oseo-Anvar France, 2008

7. Crnojevic, C., Decool, F., P. Florent - *Swirl measurements in a motor cylinder Experiments in Fluids*, 26 (1999) 542-548, Springer-Verlag
8. Fontana, G., Galloni, E. - *Variable valve timing for fuel economy improvement in a small spark-ignition engine*, Applied Energy 86 (2009) 96-105
9. Hara, V., Clenci, A. - *Adaptive Thermal Engine with Variable Compression Ratio and Variable Intake Valve Lift*, Published by University of Pitesti, ISBN 973-8212-92-8, 2002, Romania
10. Heywood, J.B.- *Internal Combustion Engine Fundamentals* ISBN 0-07-028637-X, 1988
11. Iorga-Simăn, V., Clenci, A., Podevin, P., Descombs, G. – *On the effects of the valve lifting height upon filling process*, Scientific Bulletin, University of Pitesti, 2010
12. Jorge, M., Ribeiro, B., Senhorinha, T. - *In cylinder swirl analysis of different strategies on over-expanded cycles*, International Congress of Mechanical Engineering, November 15-20, 2009, Gramado, RS, Brazil,
13. Meyer, J., - *Engine Modeling of an Internal Combustion Engine With Twin Independent Cam Phasing*, Doctoral Thesis, The Ohio State University, 2007
14. Fluent 6.2. User's guide. Fluent Inc.